Properties of high-temperature melts using levitation*

Paul C. Nordine[†], J. K. Richard Weber, and Johan G. Abadie

Containerless Research, Inc., 906 University Place, Evanston, Illinois 60201, USA

Abstract: Containerless conditions allow well-controlled investigation of liquids at high temperatures. Levitation methods used for this purpose are reviewed, and their application is illustrated by discussion of the properties and behavior of deeply undercooled yttrium–aluminum–oxide melts.

INTRODUCTION

Levitation techniques are useful tools for high-temperature melt property studies. They eliminate the problem of reaction with containers and allow deep undercooling of melts. The containerless conditions may be obtained by opposing gravity with a levitation force, or by allowing an entire experiment to free-fall. This paper addresses these methods and results of recent research using containerless techniques. It emphasizes research on properties of undercooled liquids of the yttrium aluminum garnet (YAG) composition, $Y_3Al_5O_{12}$, and novel products formed from yttria–alumina melts.

LEVITATION METHODS

In this section we review methods that have been applied to perform high-temperature experiments under containerless conditions. The emphasis is on experiments of long duration on liquids. A major source of interest and support for this work is in its extension to low gravity conditions where the forces required to perform containerless experiments are small. In low gravity, control of sedimentation, stirring, and convection is obtained to facilitate the study of transport properties and other investigations that require quiescent conditions.

Magnetic levitation

Most levitation methods oppose gravity by exerting a force on the surface of the sample. An exception where the force is exerted throughout the sample volume is the recently demonstrated levitation of diamagnetic materials in a magnetic field gradient [1]. A superconducting magnet was used to obtain magnetic fields up to 30 T and field gradients of –4200 T^2/m. Materials with a magnetic susceptibility more negative than $\chi_S = -2.9 \times 10^{-9}$ m^3/Kg were levitated. The method is applicable, for example, for levitation of H_2O, SiO_2, B_2O_3, and Al_2O_3. Experiments with levitation and laser beam heating and melting of BK7 glass showed that χ_S increases with temperature.

Electromagnetic levitation (EML)

EML, patented by Muck in 1923 [2], is one of the oldest techniques for containerless experiments. A typical EML coil has reversed winding of upper and lower sections energized by an RF power supply.

[†]Corresponding author: E-mail: pnordine@containerless.com

The EM frequency must be large enough that the EM skin depth is less than the sample radius, typically 200–400 kHz for 5-mm-diameter metallic samples.

The levitation force is proportional to the gradient, dB^2/dz, in the magnetic field intensity, and the heat input is proportional to B^2 averaged over the sample surface. An EM levitated sample thus achieves a high temperature that depends on sample density and the force of gravity. Molten samples are deformed and stirred by the EM forces.

The TEMPUS (Tiegelfreies ElektroMagnetisches Prozessieren Unter Schwerlosigkeit) facility is an electromagnetic heating and positioning system for containerless experiments in microgravity. TEMPUS employs a low-power quadrupole coil to control sample position and a higher power dipole coil for heating. Heating and positioning are not coupled, and the temperature range for containerless experiments is greatly expanded. The TEMPUS team [3] has reported experiments performed with this facility during the International Microgravity Laboratory Mission 2 (IML-2). The experiments included undercooling of liquid metals and alloys, statistics for nucleation of crystalline phases from undercooled melts, glass formation, and measurement of properties such as viscosity, surface tension, and specific heat.

Electrostatic levitation (ESL)

ESL was developed by Rhim *et al*. [4] for microgravity experiments. An advanced ESL is described by Rulison *et al*. [5]. This instrument is installed at NASA's Marshall Space Flight Center in Alabama and used in ground-based research under containerless and high vacuum conditions. Until recently, research with the ESL has emphasized work on metals such as zirconium and deep eutectic alloys, and silicon, which exhibit relatively low vapor pressures at the melting point. Recent advances have been made in the levitation and heating of oxide glasses and ceramics [6]. Surface tension and viscosity measurements under containerless conditions in an ESL, were reported by Rhim *et al*. [7].

Electric fields on the order of 1 kV/mm are used to levitate electrically-charged samples in the ESL and electrical discharges prevent operation in a gas environment. In principle, operation in low gravity can reduce the required field strength, allowing the use of an ambient gas atmosphere, investigation of more volatile materials, and studies of gas/liquid reactions and equilibria. A low-gravity ESL for the Space Station is under development by NASDA in Japan.

Gas film levitation (GFL)

GFL was first developed by Granier and Potard [8]. They report experiments to levitate and melt up to 10 g of Cu, Ag, and Au, and 2–4 g of Al and Ge. The sample is levitated by floating on a thin gas film formed by gas flow through a porous membrane. A furnace or EM-heated graphite susceptor may be used to achieve high temperatures.

Barbé *et al*. [9] used GFL to measure viscosity by a shape-relaxation method. A sample of levitated liquid was compressed by a gas film piston and then allowed to relax toward a more spherical shape under the action of surface tension forces. The quotient of viscosity and surface tension was derived from the measurements of sample shape given by the ratio of polar to equatorial radii. Viscosity values from 26 to 1.4×10^4 Pa·s were measured for a silicate glass (Schott AR glass) in the temperature range 1074–1398 K.

Aerodynamic levitation

Aerodynamic forces can be used to suspend a sample material in a gas stream that flows from a nozzle. Solid sample spheres may be levitated and laser beam heated in low-pressure free jets [10]. This method has been used in combination with laser-induced fluorescence to obtain accurate vapor pressure and melting point measurements for pure boron [11], for which no suitable container was available.

However, free-jet levitation becomes unstable when the samples are melted. Two solutions to this problem have been developed.

Aero-acoustic levitation (AAL) [12,13] stabilizes the free-jet levitation of liquids by application of relatively small and highly localized acoustic forces that control fluctuations in the sample position. Open access to the levitated sample facilitates noncontact property measurements, two-sided laser beam heating to minimize temperature gradients in the sample, use of splat-quenching devices, etc. The AAL method has been applied primarily in studies of oxides, with the apparatus open to the atmosphere. Undercooling of molten ceramic superconductors, Al_2O_3, aluminates, and geological materials [14], vaporization of impurities from Al_2O_3, glass formation, and crystal nucleation studies are reported [15–19].

The conical nozzle levitator (CNL) is the second method to obtain stable aerodynamic levitation of liquids. The sample is supported by gas flow in a diverging conical nozzle and laser beam heated from above. Temperatures in excess of 3000 K are easily realized in 3-mm-diameter oxide specimens with 250 watts of CO_2 laser beam power. The CNL is a simple and compact device that is easily integrated within an apparatus for liquid-phase property measurements or processing experiments.

The CNL method was first used in combination with EM heating of levitated aluminum and uranium liquid [20]. Later, Coutures *et al*. [21] introduced CO_2 laser beam heating and reported numerous investigations of liquid oxides, including structural investigations by NMR and EXAFS [22–24]. Krishnan *et al*. [25] developed a CNL device for synchrotron X-ray scattering measurements. Their work on molten Al_2O_3, Y_2O_3, $Y_3Al_5O_{12}$, mullite, boron, silicon, and other liquids, and theoretical modeling of the structural results were recently reviewed by Krishnan and Price [26]. Enderby *et al*. [27] adapted the CNL apparatus for measurements of the electrical conductivity of molten Al_2O_3, Ge, and Si.

Additional investigations with the CNL method include the synthesis of glass fibers from rare-earth aluminate compositions, by fiber pulling from deeply undercooled melts [28], liquid density measurements on molten Al_2O_3 [29], and synthesis of many new oxide glass materials [21,30].

TEMPERATURE MEASUREMENT

Optical pyrometry is the preferred method for noncontact temperature measurement in containerless experiments. Emissivity corrections are required to obtain the true temperature, T, from the apparent temperature, T_a, that is measured with an optical pyrometer. For a narrow-band spectral radiation pyrometer of effective wavelength, λ, Wien's approximation to Planck's law gives the relationship between T, T_a, and the spectral emissivity, ε_λ:

$$1/T - 1/T_a = \lambda/C_2 \ln \varepsilon_\lambda \tag{1}$$

where $C_2 = 1.4388 \times 10^{-2}$ m·K. For highly absorbing materials such as liquid metals, the emissivity can be quite small, on the order of 0.1 to 0.4, and emissivity corrections are large. Krishnan [31,32] developed ellipsometric measurements on levitated liquids that provide the required emissivity values.

For weakly absorbing opaque materials, such as oxide liquids at high temperatures, the normal spectral emissivity, ε_λ, is calculated from the index of refraction, n_λ, as follows:

$$\varepsilon_\lambda = 1 - [(n_\lambda - 1)/(n_\lambda + 1)]^2 - \tau_\lambda \tag{2}$$

where τ_λ is the optical transmission which equals zero for an opaque sample. For example, the value of n_λ for molten yttria–alumina compositions is approximately 1.8 at $\lambda = 650$ nm, which yields $\varepsilon_\lambda = 0.92$ and a relatively small emissivity correction to apparent temperatures. Further, n_λ typically exhibits a weak variation with temperature and wavelength, so that the total hemispherical emissivity for oxide liquids varies little with temperature, and can often be estimated to about ±5%.

The principal problem in temperature measurement on levitated oxide liquids arises at lower temperatures where the liquid begins to become transparent (i.e., τ_λ becomes significant). The emissivity is then unknown unless *in-situ* optical transmission experiments are performed. Alternatively, a different pyrometer may be used to make measurements at a wavelength at which the sample is opaque. Significant transparency (at 650 nm) begins to occur at temperatures below about 1500 K for molten yttria–alumina compositions.

RESEARCH ON UNDERCOOLED MOLTEN YAG

Yttrium aluminum garnet, $Y_3Al_5O_{12}$ or "YAG", is a technologically important material as a host crystal for Nd:YAG lasers and for potential structural applications based on its extreme resistance to creep at high temperatures. Crystal growth is known to encounter difficulties in phase selection between the garnet phase and a metastable mixture of $YAlO_3$ and Al_2O_3 [33]. The vapor pressure of YAG is quite low at the melting point (2240 K), which makes it an attractive material for containerless melt processing research. Extremely deep undercooling of the melt is possible under containerless conditions, and considerable research has been performed to investigate the properties of the liquid. In this section, we review this research which is exemplary of novel experiments that levitation methods permit.

Fragile liquids

The concept of *fragile* liquids, introduced by Angell [34], is of considerable interest in connection with oxide melts. Fragile liquids display (i) substantially greater heat capacity than the corresponding crystalline solid, and (ii) highly non-Arhennian temperature dependence of viscosity. For example, the viscosity of molten YAG is illustrated in Fig. 1, and compared with the *strong* liquid, SiO_2.

Three different experiments yield the viscosity, η, vs. temperature data in Fig. 1. The first is direct measurements at 2240–2340 K at temperatures above the melting point where $\eta \approx 0.04$ Pa·s [35]. The second is an estimated viscosity of 30–300 Pa·s at 1600–1650 K, the temperature at which glass fibers
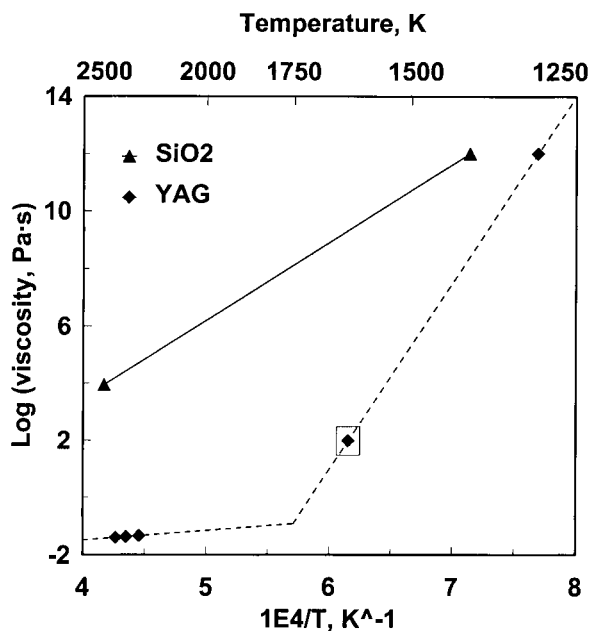

Fig. 1 Viscosity vs. temperature for a strong liquid, SiO_2, and a fragile liquid, molten $Y_3Al_5O_{12}$.

can be pulled from the undercooled liquid [28]. The third is a value of 10^{12} Pa·s at the estimated glass transition temperature, $T_g \approx 1300$ K [36].

The glass transition temperature, T_g, is defined as the temperature at which the heat capacity of the glassy or liquid phase displays an abrupt increase relative to the crystalline solid. If the solid–liquid heat capacity difference is substantial, the liquid will be fragile. Kauzmann [37] first discussed the thermodynamic consequences of this effect. The influence of the solid–liquid heat capacity difference [38] on the enthalpy and entropy of fusion of Al_2O_3 is illustrated in Fig. 2.

Figure 2 includes results for a hypothetical situation in which the larger value of the liquid heat capacity above T_g is assumed to continue at lower temperatures. It is seen that the entropy of fusion would then become zero at $T_K = 1050$ K, which is defined as the Kauzmann temperature. This situation is considered impossible; it follows that a lower limit on glass transition temperatures can be obtained from the heat capacity of the undercooled liquid.

Glass of the YAG composition is formed by cooling the liquid under containerless conditions. The enthalpy of fusion of YAG [39] is 420 kJ/mol = 21 kJ/g-atom, and the enthalpy of vitrification of the glass [40] is 13.8 kJ/g-atom. Thus, a large heat capacity difference must exist between liquid and crystalline YAG, which confirms that the undercooled liquid is fragile.

Undercooling behavior of $Y_3Al_5O_{12}$

Coutures *et al.* [21] first investigated the behavior of deeply undercooled liquid $Y_3Al_5O_{12}$. They showed that three products may be formed. Spontaneous crystallization of the melt to form a metastable mix-
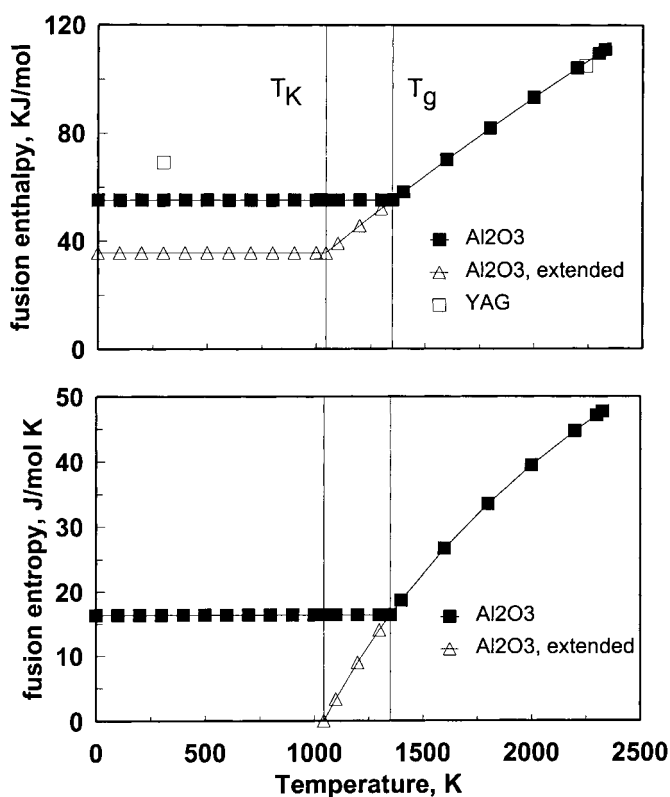
Fig. 2 Fusion enthalpy and entropy of Al_2O_3 [38] in the undercooled liquid. The enthalpies of fusion [39] and vitrification [40] of YAG are shown by open squares.

ture of crystalline $YAlO_3$ (yttrium aluminum perovskite, YAP) and $\alpha–Al_2O_3$ may occur near 1600 K, 640 K below the 2240 K melting point of crystalline YAG. Deeper undercooling leads to spontaneous crystallization to form stable crystalline $Y_3Al_5O_{12}$. Alternatively, glass is formed if the cooling rate exceeds *ca.* 200 K/s. These results have been confirmed by Nagashio and Kuribayashi [41], and in our research.

Figure 3 shows the three events that may occur upon cooling of a molten YAG sample (*ca.* 3 mm diameter) under containerless conditions. In Figs. 3A–3C, the products are a mixture of YAP and $\alpha–Al_2O_3$, glass, and YAG, respectively. Formation of crystalline products is signaled by recalescence, an abrupt temperature increase due to the enthalpy of crystallization.

The results in Fig. 3 were obtained in the aero-acoustic levitator with a levitation gas flow of pure argon gas and CO_2 laser beam heating to *ca.* 2500K prior to quenching. Apparent temperature, T_a, was measured (at temperatures below 2000 K) with a fast pyrometer whose effective wavelength was 650 nm. Figure 3 includes T_a vs. time (solid symbols), and $1/T_a^3$ vs. time (open symbols). The linear portion of $1/T_a^3$ vs. *t* shows that heat loss is primarily by radiation above 1500 K, where the liquid is opaque and the spectral and total emissivities are essentially constant. At temperatures below 1500 K, the liquid becomes increasingly transparent and the measured values of T_a fall below the fit of the data at higher temperatures.
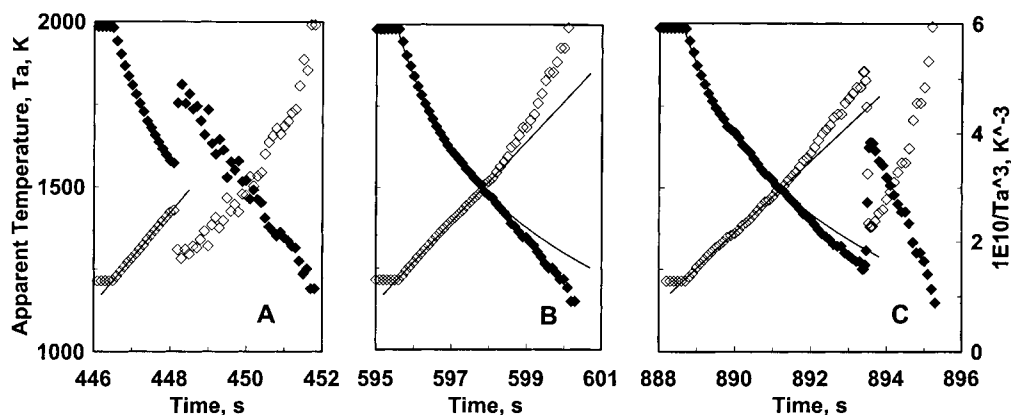

Fig. 3 Cooling curves for liquid YAG in the aero-acoustic levitator: (A) spontaneous crystallization to form $YAlO_3$ and Al_2O_3; (B) glass formation; and (C) spontaneous crystallization to form $Y_3Al_5O_{12}$.

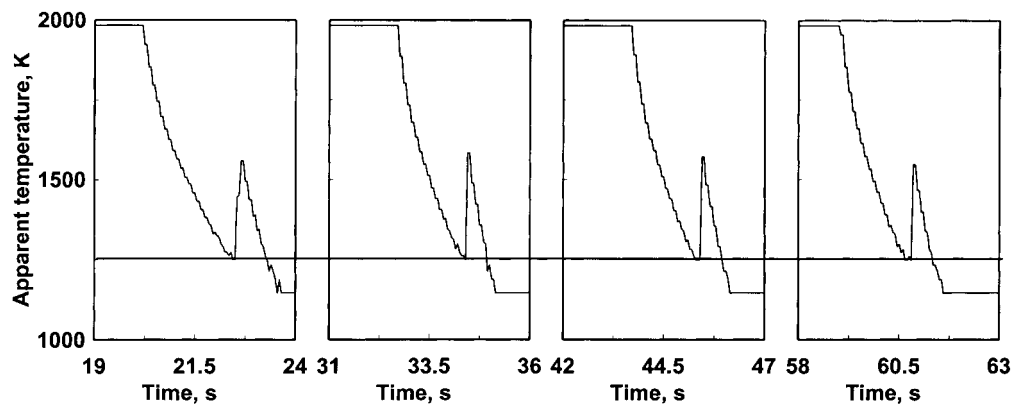**Fig. 4** Apparent temperature vs. time for molten $Y_3Al_5O_{12}$ in the conical nozzle levitator. Reproducible nucleation of crystalline YAG is observed at $T_a = 1250$ K.

Figure 4 illustrates the cooling curves obtained when a YAG sample was processed in a conical nozzle levitator. Spontaneous crystallization to form pure YAG occurred at $T_a = 1250 \pm 5$ K. If a slightly smaller sample is used in the aeroacoustic or conical nozzle levitators, the cooling rate increases, and glass is always formed upon cooling of the liquid.

The formation of YAP and α–Al_2O_3 typically occurs upon first heating and melting of a fresh sample, and reproducible crystallization to YAG, nucleated at $T_a = 1250$ K ± 5 K, occurs after the sample has been heated and cooled a few times. It is possible that loss of oxygen or moisture from a fresh sample influences the phase selection. Sensitivity to the oxygen pressure is also found by using pure oxygen as the levitation gas flow, which allows glass formation at smaller cooling rates relative to processing in argon. Crystallization of an undercooled aluminum oxide melt leads to a dendritic and porous α–Al_2O_3 in oxygen and dense prismatic crystals in argon [18]. Liquid aluminum oxide is also known to exhibit an optical absorption coefficient that varies with the ambient oxygen partial pressure [42].

Nucleation temperature

YAG nucleates from the undercooled melt at an apparent temperature, $T_{a,N} = 1250 \pm 5$ K. Since the sample is not opaque, eq. 1 yields a lower limit, $T_N(min) = 1256 \pm 5$ K on the true nucleation temperature when transparency is ignored in calculating the emissivity correction. The extrapolated fit of $1/T_a^3$ vs. t data obtained at higher temperatures yields a larger value $T_{a,N} = 1315 \pm 10$ K, averaged over several experiments. Application of the emissivity correction yields $T_N(max) = 1322 \pm 10$ K. This is an upper limit since, at lower temperatures, convective heat loss can cause a departure of the apparent temperature from the radiative cooling curve. Thus, 1256K $< T_N$(YAG) < 1322 K.

Polyamorphism in rare-earth aluminate glasses

The glass product formed from the pure YAG composition contains spheroids of one glass in a matrix of a second glass. The two glass phases are of practically identical composition. This *polyamorphism* was first described by Aasland and McMillan [36], who employed rapid cooling of liquid samples supported on an iridium filament. With containerless methods, we obtained two-phase glass materials at 23–42 mol % yttria [30]. At 28.7 mol % yttria [36], the Y:(Y+Al) composition ratios were 0.7128 $\pm$ 0.0032 (population standard deviation) for the spheroid phase and 0.7123 $\pm$ 0.0012 for the matrix phase. Our results for a pure YAG-composition glass were Y:(Y + Al) = 0.6243 $\pm$ 0.0009 for the spheroid phase and 0.6245 $\pm$ 0.0010 for the matrix phase [30]. Thus, the two glass phases have identical compositions, within approximately 0.001 in the component mol fractions.

Other rare-earth aluminate compositions form two-phase glasses under containerless cooling conditions, as shown in Table 1. Addition of lanthana to the melt resulted in single-phase glass [30].

Table 1 Single-phase and two-phase rare-earth aluminate glasses, balance Al_2O_3 . R_C measured at 1300 K under containerless conditions.

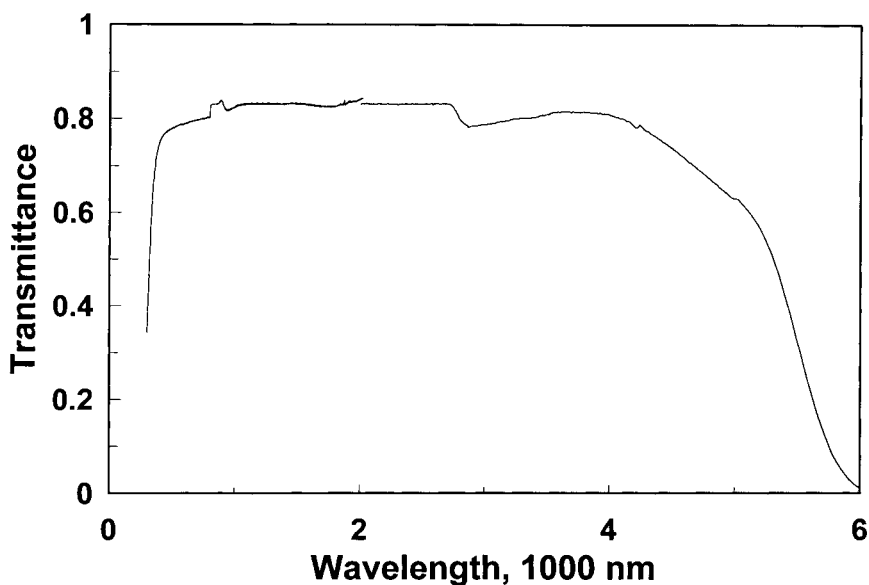| Mol % Y_2O_3	Mol % La_2O_3	Mol % Re_2O_3	Phases	R_C , K/s
23–42	0	0	2	
37.5	0	0	2	70
0	0	37.5 Lu_2O_3	2	>110
0	0	37.5 Er_2O_3	2	110
12.5	12.5	12.5 Er_2O_3	1	40
0	37.5	0	1	<40
0	50.0	0	1	<40
≤32.5	≥5	0	1	
0	5	32.5 Nd_2O_3	1	
0	7	30.5 Er_2O_3	1	

Fig. 5 Optical transmittance of $La_3Al_5O_{12}$—composition glass, 2.1-mm thickness.

Table 1 includes critical cooling rates for glass formation, R_C, which decreases with lanthana additions, allowing larger specimens of glass to be obtained. The optical transmission of a single-phase lanthanum aluminate glass is shown in Fig. 5 [43].

A two-phase $Y_3Al_5O_{12}$ composition glass gave Vickers hardness equal to 1000 and 900 on the spheroid and matrix glasses, respectively. The indenter caused cracks in the spheroid phase suggesting that the hardness value exceeds the derived result.

Structure of aluminate liquids

Coutures *et al.* [22] performed NMR measurements on aluminate liquids levitated in a CNL, to show that the concentration of 4-coordinated Al^{3+} ions is 60%, 80%, and 95% in liquid Al_2O_3, YAG, and $CaAl_2O_4$, respectively, the balance being 5- and 6-coordinated. This trend is consistent with increasing 4-coordination of Al^{3+} with the size of the added metal ion. Since La^{3+} is the largest rare-earth ion, it appears that the formation of single-phase glasses at a lower R_C relative to lanthana-free melts arises from an increase in the concentration of 4-coordinated Al^{3+} ions.

Weber *et al.* [44] performed X-ray scattering on molten YAG levitated in a CNL. They obtained radial distribution functions and mean first-shell coordination of Al^{3+} and Y^{3+} ions at temperatures from 1768–2227 K (i.e., from 472 to 13 K below the 2240 K melting point of crystalline YAG). Radial distribution function peaks were at $r \approx 1.80$ Å for Al–O and $r \approx 2.25$ Å for Y–O, consistent with 4- and 6-coordination, respectively. In pure argon the Al–O distance and coordination number increased with undercooling. EXAFS measurements on molten YAG [23,24] indicate a decrease in the mean Y–O coordination number from 8 in YAG to 7.4 in the melt.

SUMMARY

Levitation techniques are a practical means for laboratory investigations of molten materials at very high temperatures, free from contamination by containers, in highly nonequilibrium conditions, under controlled temperature and ambient pressure, and with good optical access to specimens for noncontact

property measurements. X-ray scattering, ellipsometry, drop oscillation, and shape relaxation studies have allowed structural, optical property, surface tension, and viscosity measurements on the liquid state. Deep undercooling under containerless conditions has allowed crystal nucleation, phase selection, liquid–liquid phase transitions, glass formation, and other phenomena to be investigated. The impact of levitation methods has been strong in the study of fragile liquids such as molten YAG, which displays a low viscosity at the melting point and highly non-Arhennian change of viscosity with temperature in the undercooled state. Remaining challenges for levitation hardware include the control of sample temperature gradients in laser beam heating techniques and control of fluid motion to allow high-precision transport property measurements. An apparatus for microgravity experimentation is under development that employs beam heating and electrostatic positioning with potential to meet these challenges.

ACKNOWLEDGMENTS

REFERENCES

1. N. Kitamura *et al. Jpn. J. Appl. Phys*. **39**, L324–L326 (2000).
2. O. Muck. German patent no. 42204 (Oct. 30, 1923).
3. Team TEMPUS. In *Materials and Fluids Under Low Gravity, Proc. IXth Symp. on Gravity-Dependent Phen. in Physical Sciences*, L. Ratke *et al.* (Eds.), Springer (1995).
4. W.-K. Rhim *et al. Rev. Sci. Instrum.* **54**, 307–317 (1985).
5. A. J. Rulison, J. L. Watkins, B. Zambrano. *Rev. Sci. Instrum.* **68**, 2856–63 (1997).
6. Jan Rogers. NASA Marshall Space Flight Center, private communication, March 2000.
7. W-K. Rhim, K. Ohsaka, P-F. Paradis. *Rev. Sci. Instrum.* **70**, 2796–2801 (1999).
8. J. Granier and C. Potard. In *Proc. 6th Eur. Symp. Micrograv. Bordeaux, France*, ESA SP-256 (1987), pp. 421–25.
9. J.-Ch. Barbe *et al. Int. J. Thermophys.* **20**, 1071–83 (1999).
10. P. C. Nordine and R. M. Atkins. *Rev. Sci. Instrum.* **53**, 1456 (1982).
11. S. Krishnan *et al. High Temp. Science* **31**, 45 (1991).
12. J. K. R. Weber *et al. Rev. Sci. Instrum.* **65**, 456–465 (1994).
13. J. K. R. Weber *et al. J. Jpn. Soc. Microgravity Appl.* **13**, 27–35 (1996).
14. R. F. Cooper. *et al. Science* **274**, 1173–76 (1996).
15. J. K. R. Weber *et al. J. Am. Ceram. Soc.* **76** 9., 2139–41 (1993).
16. J. R. Olive *et al. J. Mater. Res.* **9**, 1–3 (1994).
17. J. K. R. Weber *et al. J. Mater. Res.* **9**, 1657–1660 (1994).
18. J. K. R. Weber *et al. J. Am. Ceram. Soc.* **78**, 577–582 (1995).
19. A. B. Biswas, J. K. R. Weber P. C. Nordine. *J. Mat. Res.* **10**, 1823–27 (1995).
20. D. A. Winborne *et al. Metall. Trans.* **7B**, 711 (1976).
21. J. P. Coutures *et al.* In *Proc. 6th European Symposium on Materials Sciences Under Microgravity Conditions,* Bordeaux, France, 2–5 December, 1986, pp. 427–30.
22. J.-P. Coutures *et al. C. R. Acad. Sci. Paris* **310**, Série II. 1041–45 (1990).
23. X. Launay *et al. C. R. Acad. Sci. Paris*, **324**, Série II, 527–35 (1997).
24. C. Landron *et al. Europhys. Lett.* **44**, 429–435 (1998).
25. S. Krishnan *et al. Rev. Sci. Instrum.* **68**, 3512–3518 (1997).
26. S. Krishnan and D. L. Price. *J. Phys.: Condens. Matter* **12**, R145–R176 (2000).
27. J. E. Enderby *et al. Appl. Phys. Lett.* **71**, 116–118 (1997).
28. J. K. R. Weber, J. J. Felten, B. Cho, P. C. Nordine. *Nature* **393**, 769–771 (1998).
29. B. Glorieux *et al. Int. J. Thermophys.* **20**, 1085–94 (1999).

30. J. K. R. Weber *et al. J. Am. Ceram. Soc.* **83**, 1868–72 (2000).
31. S. Krishnan. *Thermophysical and Optical Property Measurements of Electromagnetically Levitated Liquid Metals*, Ph.D Thesis, Rice University, 1989.
32. S. Krishnan *et al. High Temp. Sci.* **29**, 17 (1990).
33. J. L. Caslavsky and D. J. Viechnicki. *J. Mat. Sci.* **15**, 1709–18 (1980).
34. C. A. Angell. *Science* **267** 1624–35 (1995).
35. V. J. Fratello and C. D. Brandle. *J. Cryst. Growth* **128**, 1006–1010 (1993).
36. S. Aasland and P. F. McMillan. *Nature* **369**, 633–639 (1994).
37. W. Kauzmann. *Chem Rev.* **43**, 219–56 (1948).
38. M. W. Chase, Jr., *et al. JANAF Thermochemical Tables Third Edition, J. Phys. Chem Ref. Data* **14** (1985).
39. M. Gervais *et al. J. Am. Ceram. Soc.* **75**, 3166–68 (1992).
40. I-Ching Lin *et al. J. Non-Cryst. Solids* **243**, 273–276 (1999).
41. K. Nagashio and K. Kuribayashi. *J. Mat. Res.* In press.
42. J. K. R. Weber *et al. J. Am. Ceram. Soc.* **78**, 583–587 (1995).
43. J. K. R. Weber, *et al. J. Appl. Phys.* Submitted for publication, Jan. 2001.
44. J. K. R. Weber *et al. Phys. Rev. Lett.* **84**, 3622–25 (2000).